Comparative Clinical Pathology (2019) 28:949–954
https://doi.org/10.1007/s00580-018-2841-z

ORIGINAL ARTICLE

Inorganic nanoparticles restrict viability of metastatic breast cancer cells in vitro

Oluyomi Stephen Adeyemi[1] · David Adeiza Otohinoyi[2]

Received: 21 June 2018 / Accepted: 23 October 2018 / Published online: 30 October 2018

Abstract

Available cancer therapies are limited due to undesirable side effects, non-specific cellular toxicity as well as treatment failure. Therefore, there is urgent need for newer treatment strategies. In this study, we comparatively determined the in vitro anti-cancer potential of inorganic nanoparticles (NPs) in MDA-MB-231 cancer cells. Flow cytometry, confocal microscopy, and reactive oxygen species (ROS) assays were employed to probe likely mechanism of anti-cancer action of NPs. Study demonstrated dose-dependent toxicity of NPs to MDA-MB-231 cells. The NPs promoted production of ROS and might have caused early apoptotic clearance of MDA-MB-231 cells. Considered together, the findings support anti-cancer potential of inorganic NPs. Furthermore, preliminary evidence suggests that the anti-cancer potential of these NPs may be linked with capacity to cause ROS production as well as cellular apoptosis. Further studies to clearly define the mechanistic cellular actions of these nanoparticles are warranted.

Keywords Apoptosis · Cellular death · Nanomedicine · Toxicity

Introduction

Aside lung cancer, breast cancer is a leading cause of death in women (Center for Disease Control and Prevention 2018). The likelihood of women dying from breast cancer is put at 1 in 38 (American Cancer Society 2018). As a result, there are aggressive research efforts and measures targeted at reducing cancer-related mortality. Some of these measures include early diagnosis of breast cancer, chemotherapy, radiotherapy, surgery, hormonal therapy, and more recently, targeted therapy, which involves the inhibition of growth factors on tumor cells (Thoidingjam and Tiku 2017; Moses et al. 2016; Wang et al. 2017). However, all of the current treatment strategies have yet to produce the desired outcome. In addition, there are cases of undesirable side effects with increased chances of the malignant cells developing resistance to the available therapy (Wang et al. 2017), thus making current therapeutic methods unreliable.

✉ Oluyomi Stephen Adeyemi
yomibowa@yahoo.com

[1] Medicinal Biochemistry, Nanomedicine & Toxicology Laboratory, Department of Biochemistry, Landmark University, Ipetu Road, Omu-Aran 251101, Nigeria

[2] All Saints University, School of Medicine, Hillsborough Street, Roseau, Commonwealth of Dominica

Perhaps, the limitations of available cancer therapies underscore the continuing efforts for exploring available avenue to identify better treatment strategy for breast cancer. Lately, the application of nanoparticles (NPs) for biomedical purposes including cancer therapy has been receiving wider attraction. This is because the small size of NPs gives them the ability to attain quantum dimensions with associated characteristics, thus, possessing distinctive electronic, photochemical, magnetic, chemical, and optical properties (Kumar and Yadav 2009). Previous studies have demonstrated the cytotoxic effect of NPs on human breast cancer cell lines, specifically, MDA-MB-231 human isolates (Azizi et al. 2017; Gurunathan et al. 2013; Krishnaraj et al. 2014; Wang et al. 2017). Some of the NPs with implication for breast cancer therapeutic potential include iron and palladium NPs (Thoidingjam and Tiku 2017; Yuan et al. 2017). Furthermore, investigations have revealed the apoptotic-inducing tendency of albumin-coated copper and cadmium NPs in MDA-MB-231 (Azizi et al. 2017, 2018). In addition, gold NPs (AuNPs) conjugated with *Boswellia sacra* and *Commiphora myrrha* extracts was recently reported for toxicity against MDA-MB-231 and MCF-7 cells (Moses et al. 2016). Likewise, silver NPs (AgNPs) produced from *Bacillus funiculus* were indicated for growth inhibition of MDA-MB-231 cells (Gurunathan et al. 2013). In the present study, we comparatively evaluated the cytotoxic action of Ag, Au, and Ag/AuNPs alloy in MDA-MB-231 cells.

Materials and methods

Materials

The nanoparticles (Au, Ag, and Ag/AuNPs) were gifted by a nanomedicine and biomedical research group, Department of Biochemistry and Microbiology, Rhodes University, Grahamstown, South Africa. The procedures for preparation and characterization are as previously reported elsewhere (Adeyemi and Whiteley 2013, 2014). All other reagents were of analytical grade and used as supplied.

Assay for viability of cells

MDA-MB-231 cells (ATCC®, USA) were maintained in culture media containing Dulbecco's Modified Eagle Medium (DMEM), glutamine (2 mM final concentration; Gibco, Invitrogen, UK), 5% (*v*/*v*) fetal calf serum (Gibco, Invitrogen, UK), and penicillin/streptomycin (100 U/ml; Biowhittaker, UK) and incubated at 37 °C and 5% CO_2 atmosphere. Cells were grown to 70% confluence, collected by centrifugation and seeded at a density of 6×10^4 cells per well in a 96-well plates. After overnight incubation, graded doses (0–100 μM) of NPs prepared in culture medium were added to the wells. The culture medium without NPs was added to the negative control well. After a 96-h incubation, viability of cell was determined by MTT assay (Roche Diagnostics, South Africa) as per the manufacturer's instructions. The absorbance reading was recorded at 595 nm on a microplate reader (Biotek Epoch, USA). The cell viability was determined relative to negative control cells, arbitrarily taken as 100%. The biological assay was performed separately three times and in triplicate.

Determination of reactive oxygen species (ROS) in cells

The level of ROS was determined in cells as previously described (Warleta et al. 2011). The assay depends on the oxidation of dichlorodihydro- fluorescein diacetate (DCFH-DA, Molecular Probes, USA) to dichlorofluorescein (DCF), a fluorescent compound. Briefly, cells were seeded at a density of 5×10^4 cells per well in 96-well plates and incubated overnight. Thereafter, cells were treated with graded doses (0–100 μM) of NPs. After 24-h incubation, the culture medium was removed and PBS containing DCFH-DA (100 μM final concentration) was added. After a 30-min incubation at 37 °C, fluorescence was recorded on a fluorometer (BioRAD, USA). Excitation was set at 485 and emission at 530 nm.

Apoptosis detection in MDA-MB-231 cells

The cellular apoptosis was detected by using apoptosis detection kit (Annexin V - FITC; Santa Cruz Biotech. Inc., Heidelberg, Germany) and following manufacturer's instructions. Briefly, MDA-MB-231 cells were seeded on a sterile glass coverslip at a density of 5×10^4 cells/mL. After overnight incubation, NPs (100 μM final concentration) and a MEK inhibitor, U0126 (apoptosis positive control) were added and incubation continued for additional 36 h. Thereafter, cells were stained with Annexin V and Hoescht 33342 (Sigma Aldrich, St. Louis, MO, USA) and the coverslips air dried. Capturing of stained nuclei was performed on a confocal laser microscope (Zeiss LSM 510, Germany) and analyzed using Zen software (Zeiss Inc. Germany).

Annexin V and PI apoptosis analysis of cells

The MDA-MB-231 cells were seeded at 1×10^5 cells/mL in a 12-well plate. After overnight incubation, cells were dosed with NPs (100 μM final concentration) prepared in culture medium and incubation continued for additional 24 h. Then, cells were collected by centrifugation and stained for apoptosis detection and quantification by using apoptosis detection kit (Santa Cruz Biotech. Inc., Heidelberg, Germany) and following the manufacturer's instructions. Briefly, cells were washed in cold PBS and re-suspended in 1× binding buffer at 1×10^6 cells/Ml. Thereafter, 5 μL FITC annexin V and PI were added and cells were gently vortexed and incubated in the dark. After 15 min, 400 μL 1× binding buffer was added to each sample, and analysis was performed on a FACS Aria III flow cytometer (BD Biosciences, USA). A total of 10,000 events were acquired for each sample. The unstained cells and cell samples stained with one marker only were used to set fluorescence compensations for each assay, and all data acquired by flow cytometry were analyzed with FlowJo software.

Statistical analysis

Data were analyzed by a one-way analysis of variance (GraphPad Prism 5, USA). Mean values were compared by using a Dunnett Post-hoc test. Concentrations of the NPs that reduced cell viability by 50% (i.e., EC_{50} value) was estimated from a dose-response curve and the curve fitted with a non-linear regression analysis. The results are presented as mean ± standard error of mean (SEM). Values at $p < 0.05$ are taken as significant.

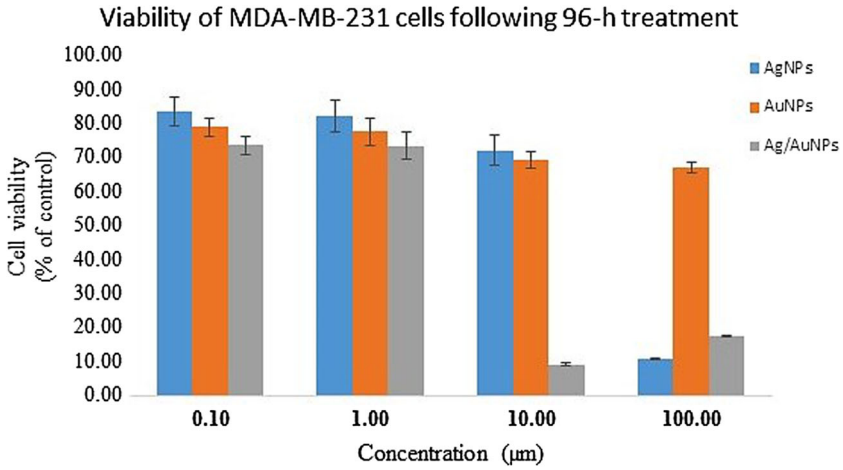

Fig. 1 Viability of human MDA-MB-231 breast cancer cells in the presence of nanoparticles. Viability of cells was determined by using a MTT reagent kit (Roche Diagnostics, South Africa). The data represent the means of three independent experiments ± SEM (standard error of mean)

Results

The cellular viability of MDA-MB-231 in the presence of Ag, Au, and Ag/AuNPs at different concentrations was determined in triplicates following 96-h incubation (Fig. 1). NPs dose dependently reduced cell viability. The cytotoxicity by NPs was observed at all doses and while AuNPs showed moderate cellular toxicity, Ag and Ag/AuNPs exhibited pronounced toxicity at higher doses. The IC_{50} (dose that inhibit 50% growth of MDA-MB-231 cells) was estimated from the dose-response curve as 2.61, 13.89, and 1.12 μM for Ag, Au, and Ag/AuNPs, respectively.

The production of ROS due to NPs in MDA-MB-231 cells was measured by fluorescence after 24-h treatment (Fig. 2a–c). In order to compare the influence of the metal NPs on the generation of ROS in MDA-MB-231 cells, the fluorescence gradient was calculated and plotted (Fig. 2d). Together, Ag, Au, and Ag/AuNPs caused significant production of ROS by MDA-MB-231. Viability of NPs-treated cells after ROS determination was ≤ 50% (Fig. 2e) thus suggesting ROS interplay in the cytotoxic action of NPs. Further, when treated cells were observed under light microscope, distortion of cellular morphology and lesser cell density were observed compared with the untreated (Fig. 3a–g). NPs caused shrinkage and detachment of cells as well as reduced cell-to-cell contact compared to the untreated cells. This do not only support the reduction in viability of MDA-MB-231 cells by NPs but the impact was dose-dependent. Furthermore, cellular analysis by laser

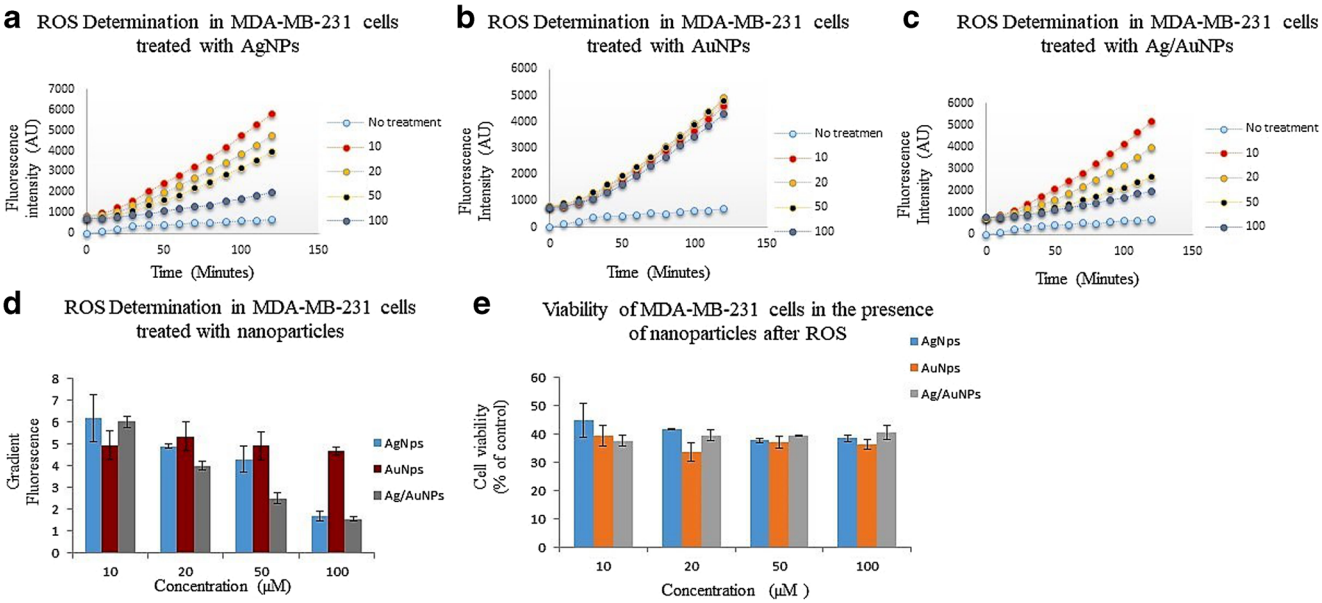

Fig. 2 Fluorescence measurement of intracellular reactive oxygen species (ROS) in human MDA-MB-231 breast cancer cells in the absence and presence of **a** AgNPs, **b** AuNPs, and **c** Ag/AuNPs. **d** Gradient fluorescence measurement of intracellular reactive oxygen species (ROS) in human MDA-MB-231 cells exposed to nanoparticles. **e** Cell viability after ROS measurement. Fluorescence was measured using a spectrofluorometer with excitation at 485 and emission at 530 nm. The data represent the means of three independent experiments ± SEM (standard error of mean)

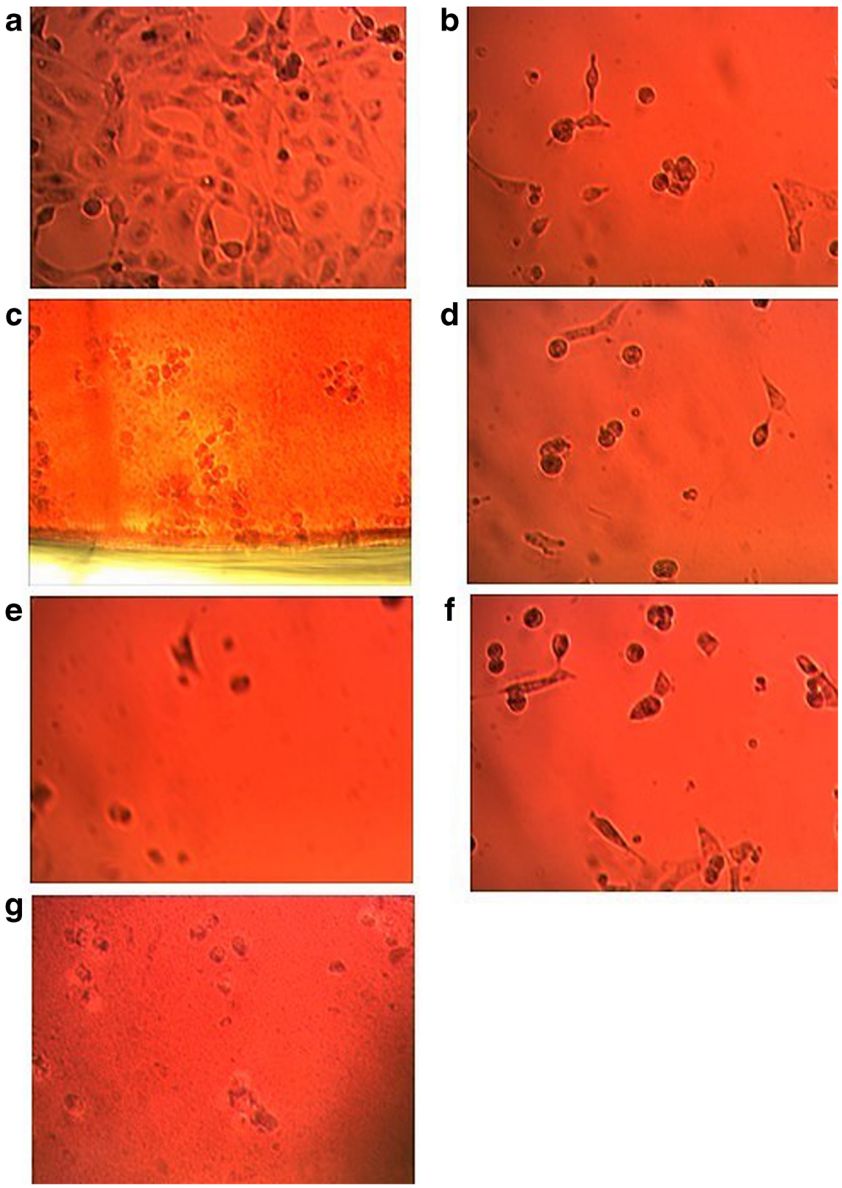

Fig. 3 Light microscopy of MDA-MB-231 breast cancer cells in the absence and presence of nanoparticles. **a** Untreated cells. **b** 10 μM AgNPs. **c** 100 μM AgNPs. **d** 10 μM AuNPs. **e** 100 μM AuNPs **f** 10 Ag/AuNPs. **g** 100 Ag/AuNPs

microscopy revealed mild apoptosis caused by NPs relative to the untreated control (Fig. 4a–e). Quantitatively, the apoptotic percentage caused by Ag, Au, and Ag/AuNPs was 3.33 ± 1.67, 3.6 ± 1.59, and 36.43 ± 8.73, respectively. The apoptotic

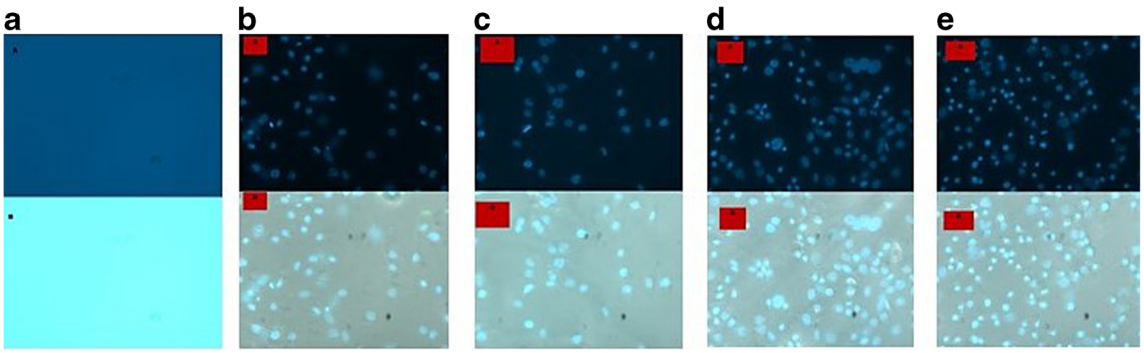

Fig. 4 Fluorescence measurement by confocal microscopy of stained human MDA-MB-231 cells. **a** Untreated cell (negative control) no staining. **b** MEK inhibitor (U1026) treated (positive control). **c** AgNPs treatment. **d** AuNPs treatment. **e** AgAuNPs treatment. Top panels show the total number of cells (Hoescht 33342 staining) while the bottom panels show the apoptotic cells (Annexin V staining)

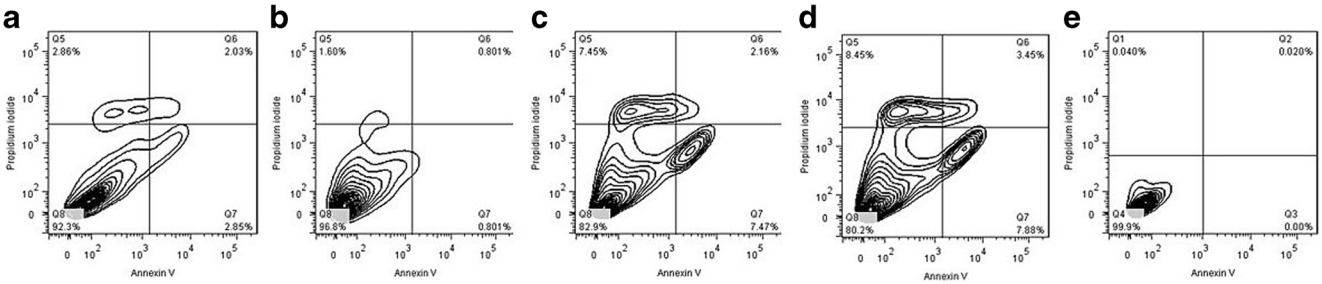

Fig. 5 Flow cytometry analysis of MDA-MB-231 cells. **a** Untreated but stained—no significant level of apoptosis observed. **b** AgNPs treated—demonstrates early apoptosis. **c** AuNPs treated—demonstrates early to mid-apoptosis. **d** Ag/AuNPs nanoparticle treated—demonstrate apoptosis. **e** Untreated and not stained—no apoptotic process observed

percentage of positive (MEK inhibitor) and negative control was 50.47 ± 5.40 and 4.7 ± 0.82, respectively. In addition, analysis of treated cells by flow cytometry confirmed the tendency of NPs to induce apoptosis in MDA-MB-231 cells (Fig. 5a–e). To validate the assay, triton X-treated cells which was included as positive control had > 23% apoptosis (data not shown).

Discussion

Reports have demonstrated the cytotoxic action of AgNPs and AuNPs against cancer cells (Gurunathan et al. 2013; Moses et al. 2016). Thus, in the current study, we comparatively evaluated Ag, Au, and Ag/AuNPs for toxicity against MDA-MB-231 cells.

The exposure of MDA-MB-231 cells to NPs appreciably caused dose-dependent reduction in cell viability in manners that suggest cellular toxicity and death. That AgNPs and Ag/AuNPs caused similar level of cellular toxicity may indicate, that AgNPs potentiated the toxic action of AuNPs in a synergistic manner. Of course, AgNPs have been implicated for higher cytotoxic action than AuNPs (Meyer 2017; Bhattacharya and Mukherjee 2008; Asharani et al. 2010). Together, our finding is consistent with investigations that demonstrated the anti-cancer potential of metal NPs including AgNPs and AuNPs (Azizi et al. 2017, 2018; Gurunathan et al. 2013; Moses et al. 2016; Yuan et al. 2017). That Ag/AuNPs caused higher cytotoxicity may indicate synergistic effect by the individual NPs. But whether the individual NPs affect similar cellular targets remain unknown and this knowledge would be necessary in order to harness fully their synergism for effective therapy. Nevertheless, our present finding support ROS production in MDA-MB-231 cells by NPs, and this might have contributed in part to the cellular toxicity. The finding conforms with reports that demonstrated the capability of metal NPs to alter the homeostasis of tumor cells by causing redox imbalance or by preventing ROS scavenging (Toyokuni et al. 1995). Similarly, Gurunathan et al. (2013) showed that AgNPs can stimulate mass production of ROS as well as induce apoptosis by activating caspase 3. Likewise, AuNPs have been implicated for ability to stimulate ROS generation (Shrivastava et al. 2014). In the present study, AgNPs and Ag/AuNPs caused higher ROS production compared with the minimal ROS generation by AuNPs treatment. Therefore, it is plausible that ROS production contributed to cellular death by the NPs. Although, for treatment with Ag/AuNPs, the observed cellular death may be associated with synergy between the individual NPs.

Furthermore, assessment for cell shrinkage, morphological modification, and cell rounding, as hallmarks of apoptosis (Duangmano et al. 2012), by light microscopic analysis revealed that exposure of MDA-MB-231 cells to NPs does not only distort cellular architecture in manners that suggest early apoptosis but also caused lower cell density. Additionally, analysis of treated cells by both the laser microscopy and flow cytometry revealed the susceptibility of MDA-MB-231 cells to apoptosis by NPs, in particular Ag/AuNPs. Meanwhile, the cellular apoptosis due to the treatment with either of AgNPs and AuNPs was comparable to that of the negative control and far less than that of the positive control (MEK inhibitor). It may therefore mean that, synergy between the individual NPs might be responsible for the cellular apoptosis by Ag/AuNPs. The NPs caused cellular apoptosis which may be associated with their capacity to promote ROS production and thus suppressing cellular viability. This is plausible if we consider that ROS production has been linked to apoptotic death of cancer cells (Gurunathan et al. 2013). Taken together, our findings do not only support that NPs caused cellular toxicity but preliminarily implicate interplay of ROS production and apoptosis, in particular by Ag/AuNPs, as contributing to the cellular death by the NPs.

In conclusion, the present study provides evidence to support the anti-cancer potential of NPs in MDA-MB-231 breast cancer cells. Both the AgNPs and AuNPs individually caused cellular death of MDA-MB-231, but the cellular toxicity was more pronounced with Ag/AuNPs treatment, and this was in manners that suggest synergy between the individual NPs. Furthermore, our data support culpability of ROS production in the cellular death caused by the NPs. Overall, findings are not only promising and supportive of medicinal prospects of NPs but also warrant further investigation to clearly define the mechanistic action involved in the cellular death by NPs.

Acknowledgements Authors acknowledge the Department of Biochemistry and Microbiology, Rhodes University, South Africa.

Compliance with ethical standards

Conflict of interest The authors declare that they have no conflict of interest.

Ethical approval This article does not contain any studies with human participants or animals performed by any of the authors.

References

Adeyemi O, Whiteley C (2013) Interaction of nanoparticles with arginine kinase from *Trypanosoma brucei*: kinetic and mechanistic evaluation. Int J Biol Macromol 62:450–456

Adeyemi O, Whiteley C (2014) Interaction of metal nanoparticles with recombinant arginine kinase from *Trypanosoma brucei*: thermodynamic and spectrofluorimetric evaluation. Biochim Biophys Acta 1840:701–706

American cancer society (2018) How Common Is Breast Cancer? https://www.cancer.org/cancer/breast-cancer/about/how-common-is-breast-cancer.html. Accessed 4 Mar 2018

Asharani P, lianwu Y, Gong Z, Valiyaveettil S (2010) Comparison of the toxicity of silver, gold and platinum nanoparticles in developing zebrafish embryos. Nanotoxicol 5:43–54

Azizi M, Ghourchian H, Yazdian F, Bagherifam S, Bekhradnia S, Nyström B (2017) Anti-cancerous effect of albumin coated silver nanoparticles on MDA-MB-231 human breast cancer cell line. Sci Rep 7:5178

Azizi M, Ghourchian H, Yazdian F, Alizadehzeinabad H (2018) Albumin coated cadmium nanoparticles as chemotherapeutic agent against MDA-MB-231 human breast cancer cell line. Artif Cells Nanomed Biotechnol 46:1–11

Bhattacharya R, Mukherjee P (2008) Biological properties of "naked" metal nanoparticles. Adv Drug Deliv Rev 60:1289–1306

Centers for Disease Control and Prevention (2018) Breast cancer in young women https://www.cdc.gov/cancer/breast/young_women/bringyourbrave/pdf/breastcanceryoungwomenfactsheet.pdf. Accessed 3 Mar 2018

Duangmano S, Sae-lim P, Suksamrarn A, Domann F, Patmasiriwat P (2012) Cucurbitacin B inhibits human breast cancer cell proliferation through disruption of microtubule polymerization and nucleophosmin/B23 translocation. BMC Complement Altern Med 12:185

Gurunathan S, Han J, Eppakayala V, Jeyaraj M, Kim J (2013) Cytotoxicity of biologically synthesized silver nanoparticles in MDA-MB-231 human breast cancer cells. Biomed Res Int 2013:1–10

Krishnaraj C, Muthukumaran P, Ramachandran R, Balakumaran M, Kalaichelvan P (2014) Acalypha Indica Linn: biogenic synthesis of silver and gold nanoparticles and their cytotoxic effects against MDA-MB-231, human breast cancer cells. Biotechnol Rep 4:42–49

Kumar V, Yadav S (2009) Plant-mediated synthesis of silver and gold nanoparticles and their applications. J Chem Technol Biotechnol 84:151–157

Meyer J (2017) Silver nanoparticles are in general more toxic to *C. elegans* than tested gold, copper, iron, titanium dioxide, zinc oxide, cerium oxide, and carbon-based nanoparticles http://wbg.wormbook.org/2017/01/17/silver-nanoparticles-are-in-general-more-toxic-to-*c-elegans*-than-tested-gold-copper-iron-titanium-dioxide-zinc-oxide-cerium-oxide-and-carbon-based-nanoparticles/. Accessed 4 Mar 2018

Moses SL, Edwards VM, Brantley E (2016) Cytotoxicity in MCF-7 and MDA-MB-231 breast cancer cells, without harming MCF-10A healthy cells. J Nanomed Nanotechnol 7:369

Shrivastava R, Kushwaha P, Bhutia Y, Flora S (2014) (2014) Oxidative stress following exposure to silver and gold nanoparticles in mice. Toxicol Ind Health 32:1391–1404

Thoidingjam S, Tiku A (2017) New developments in breast cancer therapy: role of iron oxide nanoparticles. Adv Nat Sci Nanosci Nanotechnol 8:023002

Toyokuni S, Okamoto K, Yodoi J, Hiai H (1995) Persistent oxidative stress in cancer. FEBS Lett 358:1–3

Wang W, Zhang L, Chen T, Guo W, Bao X, Wang D, Ren B, Wang H, Li Y, Wang Y, Chen S, Tang B, Yang Q, Chen C (2017) Anticancer effects of resveratrol-loaded solid lipid nanoparticles on human breast cancer cells. Molecules 22:1814

Warleta F, Quesada C, Campos M, Allouche Y, Beltrán G, Gaforio J (2011) Hydroxytyrosol protects against oxidative DNA damage in human breast cells. Nutrients 3:839–857

Yuan Y, Peng Q, Gurunathan S (2017) Combination of palladium nanoparticles and tubastatin-A potentiates apoptosis in human breast cancer cells: a novel therapeutic approach for cancer. Int J Nanomedicine 12:6503–6520